International Forum on Aeroelasticity and Structural Dynamics
IFASD 2024
17-21 June 2024, The Hague, The Netherlands

REDUCED ORDER MODELING ANALYSIS FOR FLEXIBLE WING USING A CO-ROTATIONAL BEAM ELEMENT

Yali Shao[1], Changchuan Xie[1,2*], Chao An[1], Duoyao Zhang[1], Yuhui Zhang[1]

[1] School of aeronautic science and engineering, Beihang University,
100191 Beijing, China
[2] Hangzhou International Innovation Institute, Beihang University
311115 Hangzhou, China
*xiechangc@buaa.edu.cn

Keywords: reduced order model, Harmonic Balance Method, Co-Rotational, static aeroelastic analysis

Abstract: An accurate method for large deformation structural modeling is fundamental to geometrically nonlinear aeroelasticity analysis. This paper develops a nonlinear reduced order modeling method suitable for aeroelastic analysis with high efficiency and sufficient fidelity. The structural reduced order modeling method is based on equations derived from the Galerkin approach to solve the geometric nonlinear dynamics in a weak form, in which the explicit calculation of nonlinear stiffness is not practical. Based on dynamic response data samples, nonlinear stiffness coefficients in structural dynamics equation are identified based on the fast Fourier transform and the Harmonic Balance nonlinearity identification technique. Co-Rotational finite element method is adopted for the structural simulation of a wing model to provide dynamic response data. Through static verification, the nonlinear reduced order modeling based on Co-Rotational finite element method is moderately accurate. Then, the static aeroelastic method based on reduced order modeling method coupled with vortex lattice method is established and proves its effectiveness by comparing with nonlinear finite element method coupled with vortex lattice method.

1 INTRODUCTION

High-altitude long-endurance (HALE) unmanned aerial vehicles (UAVs), exemplified by the “Helios”, have excellent application prospects in both military and civilian fields. Typically, wings of these types of aircraft need to be of large aspect ratio and high rate of composite material usage to meet the requirements for aerodynamic characteristics of high lift-to-drag ratio, which leads to low stiffness and large deformation, resulting in serious geometrically nonlinear aeroelasticity phenomenon. Structural modeling is essential to aeroelasticity analysis, and an accurate method for large deformation structural modeling is fundamental to geometrically nonlinear aeroelasticity analysis. Researchers have developed different methods for large deformation structural modeling for aeroelasticity applications. The traditional displacement-based finite element methods, Total Lagragian (TL) and Updated Lagragian (UL) method, has high applicability and mature software code, but their solution efficiency is low. The Co-Rotational method, developed for geometrically nonlinearity, deal with large deformation problem faster, but is not efficient enough for preliminary design of flexible wings and not very mature. Hodges' exact beam model, the strain-based finite element method, and the finite segment model are computationally efficient but are not convenient for handling complex models, limiting their scope of use. Structural reduced-order models can effectively reduce the degrees of freedom, improve computational efficiency, and maintain applicability to complex models.

Reduced order methods commonly used in structural dynamics analysis include static condensation (Guyan reduction), dynamic condensation, and modal reduction. Modal analysis methods in linear dynamics cannot be directly applied to geometrically nonlinear analysis and require modifications to address the characteristics of nonlinear problems. McEwan et al. [1] presented in 2001 a form of nonlinear reduced-order equations and a method for solving nonlinear stiffness coefficients suitable for large deformation structural calculations. Mignolet and Soize [2] subsequently derived the origins of the nonlinear terms. This method selects linear structural modes as the basis functions for reduction, expressing the structural dynamics equations in modal space and neglecting the transient terms, and static deformations and loads obtained from nonlinear finite element analysis are used as samples. It employs regression analysis to determine the unknown nonlinear stiffness coefficients. Compared to nonlinear displacement-based finite element methods, it significantly reduces the number of degrees of freedom and can be applied without modification to almost all commercial software, maintaining applicability to complex models.

Using structural reduced-order models, Harmin and Cooper [3] established a geometrically nonlinear aeroelasticity analysis model with the Doublet Lattice Method to analyze the nonlinear flutter problem of highly flexible wings. An et al. [4][5] considered the aerodynamic follow-on effect, improved the regression analysis method of the structural reduced-order model, and combined it with the surface vortex lattice method (VLM) to analyze the geometrically nonlinear static/dynamic aeroelastic responses of highly flexible wings. Cesnik et al. [6] integrated the structural reduced-order model into an aeroelastic framework based on a Computational Fluid Dynamics (CFD) aerodynamic program, further enhancing the accuracy of the analysis.

In the above research, the nonlinear stiffness coefficients are obtained by regression analysis in the static form of equations, requiring a huge amount of static deformation and load cases as samples, of which the time cost is high. Meanwhile, neglecting unsteady terms can result in the loss of information in the process of identifying nonlinear stiffness coefficients. In the parametric identification of nonlinear system, frequency-domain methods, such as the Discrete Fourier Transform (DFT) and the Harmonic Balance Method (HBM), and time-domain methods, such as the Restoring Force Surface (RFS) analysis and Nonlinear Subspace Methods, are widely used for the parametric identification of nonlinear system by dynamic response samples. However, such methods are rarely used in the identification of stiffness coefficients of geometrically nonlinear structure.

The dynamic response data, used in the parametric identification, can be collected by the mature finite element methods of the commercial software, such as UL and TL adopted in the Nastran/Abaqus, however, these traditional displacement-based finite element methods converge slow and difficultly when processing nonlinear deformation problems. In comparison, CR(Co-Rotational) method is specially developed for dealing with geometrically nonlinear deformation.

In this paper, we establish the geometrically nonlinear structural dynamics equations, and identify the nonlinear stiffness coefficients using the Harmonic Balance Method based on the dynamic response samples, and the reduced ordered model for flexible wings are obtained. The dynamic response samples are obtained by CR finite element. Compared with the traditional nonlinear element method, the accuracy of the reduced order model is verified. The static aeroelastic system, combining the reduced order model and the vortex lattice method, is established and the result show that the reduced order model is applicable in the static aeroelastic analysis.

2 METHOD

2.1 Reduced order model (ROM)

Geometrically nonlinear problems have the same characters: large global displacement with still small local strain, which means that the relationship between displacement and strain is nonlinear while constitutive relationship between stress and stain is linear. Without considering structure damping and by means of momentum conservation theory, the balance equation of the structure domain is written as:

$$\frac{\partial}{\partial X_k}\left(F_{ij}S_{jk}\right)+\rho_0 b_i^0=\rho_0\ddot{u}_i \quad \boldsymbol{X}\in\mathbf{\Omega}_0 \tag{1}$$

where ρ_0 is structure density of the reference frame; b_i^0 is the body force of the element; F_{ij} is deformation gradient; S_{jk} is the second P-K stress tensor; u_i is a component of node deformation ; X_k is a component of node reference position coordinate ; $\mathbf{\Omega}_0$ represents structure domain. The Einstein notation is adopted in the equation (1). On the structure domain boundary $\partial\mathbf{\Omega}_0$, surface force t^0 is imposed on boundary $\partial\mathbf{\Omega}_0^t$ while boundary $\partial\mathbf{\Omega}_0^u$ specifies the boundary displacement. Therefore, the boundary condition can be expressed as

$$F_{ij}S_{jk}n_k^0=t_i^0 \quad X\in\partial\mathbf{\Omega}_0^t \tag{2}$$

$$\boldsymbol{u}=\mathbf{0} \quad \boldsymbol{X}\in\partial\mathbf{\Omega}_0^u \tag{3}$$

In the equation (2) and (3), $\boldsymbol{n}^0$ is the unit normal vector which is vertically outward from boundary $\partial\mathbf{\Omega}_0^t$; $\boldsymbol{u}$ is the displacement vector of structure domain. Note that $\boldsymbol{b}^0$ and $\boldsymbol{t}^0$ in the equation (1) and (2) correspond to body force and surface force applied in the deformed configuration and converted to the reference configuration. Equation (1) ~ (3) are the control equations which determine the stress field and strain field of arbitrary position of structure, and equation (3) means that the boundary displacement of reference configuration is zero.

Assuming $v_i=v_i(\boldsymbol{X})$ satisfying equation (1) and $\bar{v}_i=\bar{v}_i(X)$ satisfying equation (2) and (3), the weak form of equivalent integral of equation (1) can be expressed as

$$\int_{\mathbf{\Omega}_0}\rho_0 v_i\ddot{u}_i\mathrm{d}X+\int_{\mathbf{\Omega}_0}\frac{\partial v_i}{\partial X_k}\left(F_{ij}S_{jk}\right)\mathrm{d}X=\int_{\mathbf{\Omega}_0}\rho_0 v_i b_i^0\mathrm{d}X+\int_{\partial\mathbf{\Omega}_0^t}v_i t_i^0\mathrm{d}s \tag{4}$$

Assuming $u_i(\boldsymbol{X},t)$,which is one of components of displacement field $\boldsymbol{u}$, meets:

$$u_i(\boldsymbol{X},t)=\sum_{n=1}^{M}q_n(t)U_i^{(n)}(\boldsymbol{X}) \tag{5}$$

In the equation (5), $U_i^{(n)}(\boldsymbol{X})$ is one of basis function components; $q_n(t)$ is the undetermined parameters, i.e. generalized coordinates. Approximate solutions are obtained by Galerkin method assuming $v_i = U_i^{(n)}(\boldsymbol{X}), n = 1, 2, ..., M$, of which M means the number of selected basis functions, i.e. order of the model. Substituting equation (5) into equation (4), the reduced order structure dynamic equation can be obtained by algebraic operation, which can be expressed at tensor form:

$$M_{mn}\ddot{q}_n + K_{mn}^{(1)}q_n + K_{mnl}^{(2)}q_n q_l + K_{mnlp}^{(3)}q_n q_l q_p = f_m \tag{6}$$

where M_{mn} is the mass matrix; $K_{mn}^{(1)}$, $K_{mnl}^{(2)}$, $K_{mnlp}^{(3)}$ are the stiffness matrix; f_m is the force;

The basis functions aren't restricted in the deduction of above-mentioned reduced order equations. The linear modes of structure, also known as natural modes of structure, meet the requirements of basis functions of Galerkin method and have the characteristic of being easily solved in structural analysis. Therefore, adopting linear modes as the basis functions of equation (5) is a natural and reasonable choice.

Assuming a natural mode set $\boldsymbol{\Phi} = \{\boldsymbol{\Phi}_1, \boldsymbol{\Phi}_2, \cdots, \boldsymbol{\Phi}_M\}$, the basis function can be expressed as

$$\boldsymbol{U}^{(m)} = \boldsymbol{\Phi}_m \tag{7}$$

Substituting equation (13) into equation (7) and (8) and considering orthogonality of natural modes, a generalized mass term M_{mn} and generalized stiffness term $K_{mn}^{(1)}$ can be obtained

$$\begin{cases} M_{mn} = \bar{M}_m & m = n \\ M_{mn} = 0 & m \neq n \end{cases} \tag{8}$$

$$\begin{cases} K_{mn}^{(1)} = \bar{K}_m & m = n \\ K_{mn}^{(1)} = 0 & m \neq n \end{cases} \tag{9}$$

where $\bar{M}_m$ is a generalized mass term and $\bar{K}_m$ is a generalized stiffness term.

The relationship between physical displacement and generalized coordinate ca be expressed

$$q_m = \frac{\mathbf{\Phi}_m^{\mathrm{T}}\boldsymbol{M}\mathbf{u}}{\bar{M}_m} \tag{10}$$

where $\boldsymbol{M}$ is a physical mass matrix of structure.

Equation (6) can be simplified as

$$\bar{M}_m\ddot{q}_m + \bar{K}_m q_m + K_{mnl}^{(2)}q_n q_l + K_{mnlp}^{(3)}q_n q_l q_p = f_m \tag{11}$$

where nonlinear stiffness coefficients $K_{mnl}^{(2)}$ and $K_{mnlp}^{(3)}$ are undetermined parameters of reduced order model.

2.2 Nonlinear coefficients identification

The frequency domain parameter identification method for multi-freedom nonlinear system based on Harmonic Balance Method is adopted to identify nonlinear ftiffness coefficients $K_{mnl}^{(2)}$ and $K_{mnlp}^{(3)}$. By discretizing the generalized coordinate response q_m and generalized force f_m at equal time intervals, we can obtain that

$$\bar{M}_m \ddot{q}_m(i) + \bar{K}_{mn} q_m(i) + K^{(2)}_{mnl} q_n(i) q_l(i) + K^{(3)}_{mnlp} q_n(i) q_l(i) q_p(i) = f_m(i) \tag{12}$$

where $i = 1, 2, ..., N$, and N is the total number of time discretization. The generalized coordinate response q_m is discrete Fourier transformed to $Q_m(k), k = 1, 2, \cdots, L$, and L is the total number of frequency discretization. $Q_m(k)$ meet the equation

$$Q_m(k) = \sum_{i=0}^{N-1} q_m(i) \mathrm{e}^{-\frac{\mathrm{j}2\pi ik}{N}} \tag{13}$$

Similarly, $\ddot{q}_m(i)$, $q_n(i) q_l(i)$, $f_m(i)$ of equation (18) are discrete Fourier transformed to the following frequency sequence

$$\hat{Q}_m(k) = \sum_{i=0}^{N-1} \ddot{q}_m(i) \mathrm{e}^{-\frac{\mathrm{j}2\pi ik}{N}} \tag{14}$$

$$Q^{(2)}_{nl}(k) = \sum_{i=0}^{N-1} q_n(i) q_l(i) \mathrm{e}^{-\frac{j2\pi ik}{N}} \tag{15}$$

$$Q^{(3)}_{nlp}(k) = \sum_{i=0}^{N-1} q_n(i) q_l(i) q_p(i) \mathrm{e}^{-\frac{\mathrm{j}2\pi ik}{N}} \tag{16}$$

$$F_m(k) = \sum_{i=0}^{N-1} f_m(i) \mathrm{e}^{-\frac{\mathrm{j}2\pi ik}{N}} \tag{17}$$

Frequency dynamic equation of structure after dicrete Fourier transformation can be expressed as

$$\bar{M}_m \hat{Q}_m(k) + \bar{K}_m Q_m(k) + K^{(2)}_{mnl} Q^{(2)}_{nl}(k) + K^{(3)}_{mnlp} Q^{(3)}_{nlp}(k) = F_m(k) \quad k = 0, 1, \cdots, L-1 \tag{18}$$

Under a given form and scale of test load, time-domain dynamic response samples $\tilde{u}$ can be calculated by nonlinear finite elment method, and then are dicrete Fourier transformed to dicrete generalized coordinate response samples $\tilde{q}_m$. Combined with equation (19) ~ (23), the frequency sequence samples $\tilde{Q}_m(k)$, $\tilde{\hat{Q}}_m(k), \tilde{Q}^{(2)}_{nl}(k), \tilde{Q}^{(3)}_{nlp}(k)$ and $\tilde{F}_m(k)$ can all be obtained.

By keeping the parts containing unknown coefficients at the left side of the equation and moving the other parts to the right side of the equation, equation (24) can be expressed in the form of regression problem as

$$K^{(2)}_{mnl} \tilde{Q}^{(2)}_{nl}(k) + K^{(3)}_{mnlp} \tilde{Q}^{(3)}_{nlp}(k) = \tilde{F}_m(k) - \bar{M}_m \tilde{\hat{Q}}_m(k) - \bar{K}_m \tilde{Q}_m(k) \quad k = 1, 2, \cdots, L \tag{19}$$

Equation (25) contains a total of L linear equations. By selecting a adequate value of L and solving the least squares solution of Equation (25), nonlinear stiffness coefficients $K^{(2)}_{mnl}$ and $K^{(3)}_{mnlp}$ can be identified.

2.3 Co-Rotational method

The essential of Co-Rotational (CR) method is to decompose nonlinear deformation into rigid body movement and linear elastic deformation. Firstly, a local Co-Rotational reference frame is defined, in which deformation is linear and elastic. Then the relationship between local and global deformation as well as between local internal force and global internal force are established. Finally, the global tangent stiffness matrix can be obtained by combining the relationships. Theoretically, CR method, which is based on existing linear elastic element types, is easier to construct and shows higher computational efficiency compared with traditional displacement-based finite element method.

2.3.1 3-D beam element

According to the principle of virtual work,

$$V = \delta \boldsymbol{p}_g^T \boldsymbol{f}_g = \delta \boldsymbol{p}_l^T \boldsymbol{f}_l \tag{20}$$

where $\boldsymbol{p}_g$ is global displacement; $\boldsymbol{p}_l$ is local displacement; $\boldsymbol{f}_g$ is global internal force; $\boldsymbol{f}_l$ is local internal force. δ represents variational symbol.

The relationship between global displacement and local displacement can be expressed as

$$\delta \boldsymbol{p}_l = \boldsymbol{B}^T \delta \boldsymbol{p}_g \tag{21}$$

In the equation, $\boldsymbol{B}$ is transformation matrix from local reference frame to global frame, which can be obtained through geometrical analysis involving 3-D rotation parameterization. Substituting equation (27) into (26), we can obtain

$$\boldsymbol{f}_g = \boldsymbol{B}^T \boldsymbol{f}_l \tag{22}$$

By differentiating equation (28), and combining with $\delta \boldsymbol{f}_g = \boldsymbol{K}_g \delta \boldsymbol{p}_g$ and $\delta \boldsymbol{f}_l = \boldsymbol{K}_l \delta \boldsymbol{p}_l$, global stiffness can be expressed as

$$\boldsymbol{K}_g = \boldsymbol{B}^T \boldsymbol{K}_l \boldsymbol{B} + \frac{\partial \boldsymbol{B}}{\partial \boldsymbol{p}_g} : \boldsymbol{f}_l \tag{23}$$

where $\boldsymbol{K}_g$ is global stiffness matrix, $\boldsymbol{K}_l$ is local stiffness matrix, colon represents omission. The first term in the right side of equation (29) is the local stiffness transformed to global reference frame, and the second term is the geometrical tangent stiffness matrix induced by deformation.

2.3.2 Time-domain dynamic analysis of CR element

Dynamic equation is

$$\boldsymbol{M}\ddot{\boldsymbol{x}} + \boldsymbol{f}_i(\boldsymbol{x}) - \boldsymbol{f}_e(\boldsymbol{x}) = 0 \tag{24}$$

where $\boldsymbol{M}$ is a mass matrix of beam element, $\ddot{\boldsymbol{x}}$ is the acceleration, $\boldsymbol{f}_i(\boldsymbol{x})$ is internal force and $\boldsymbol{f}_e(\boldsymbol{x})$ is external force.

To solve for the dynamic response result, Newmark integration method is adopted. The key is to assume the predicted value of displacement, velocity and acceleration, and correct the predicted value using Newton-Raphson iteration method.

2.4 Static aeroelastic analysis

The plane aerodynamic model, without considering surface effect of lift surface during deformation of a wing, is adopted in traditional aeroelastic analysis and has high accuracy when the deformation of a wing is small. However, for a wing with geometrically nonlinear deformation, the model is not no longer suitable, which would cause huge difference without considering surface effect. Therefore, in this paper the surface vortex lattice method [8] is adopted as aerodynamic model, and performes static aeroelastic analysis for a largely flexible wing combined with nonlinear reduced order model.

The procedure of static aeroelastic analysis is as follows:

(a) Input the model and calculating conditions;
(b) Calculate aerodynamic force by surface vortex lattice method;

(c) Interpolate force;
(d) Calculate static deformation by nonlinear reduced order model;
(e) Judge convergency through the displacement condition of $\left\| \boldsymbol{U}_{\text{Stip}}^{i+1} - \boldsymbol{U}_{\text{Stip}}^{i} \right\| < \eta$; if the result is yes, then jump to step (g); if the result is no, then proceed to step (f);
(f) Interpolate the displacement and update the aerodynamic model; go back to step (b);
(g) Output static aeroelastic results.

Here $\boldsymbol{U}_{\text{Stip}}^{i}$ is structural nodal displacement of the wing tip in the i$^{\text{th}}$ iteration step; η is the convergency criterion.

3 NUMERICAL EXAMPLE

3.1 Model

In this paper, a single-spar straight wing is adopted as a research object to study the accuracy of nonlinear reduced-order model. The original point is located at the rigid support at the root of the wing; the positive direction of x-axis points from the leading edge of the wing to the trailing edge; the positive direction of y-axis points from the root of the wing to the tip; z-axis satisfies the right-hand rule. A counterweight rod is located at the wing tip to adjust the structure deformation of the wing. The finite element model of the wing is shown as Figure 1 and the design parameters of the wing is shown as Table 1.

The results of linear modal analysis are shown as Table 2. The first mode, i.e. the first vertical bending mode, is low in the frequency, which indicates that the wing model is largely flexible. The deformation of the wing can be large under aerodynamic load.

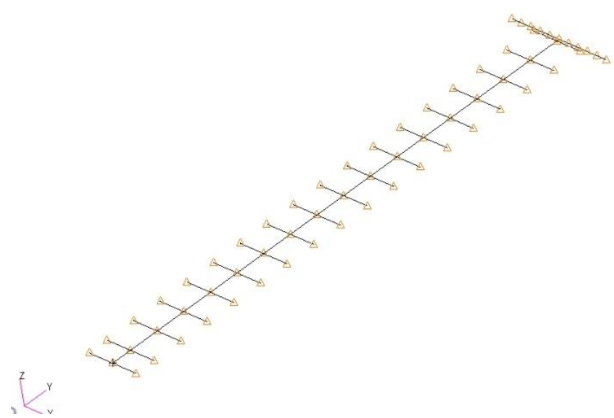

Figure 1: Finite element model.

Table 1: Design parameters of the model.

Design Parameters	value
Semispan/mm	1000
Chord Length/mm	100
Location of elastic axe	50% chord length
Density of spar/(kg·m^{-3})	7.75x10^{3}

Section shape of spar	35mmx1.5mm(rectangle)
Counterwight Rod Length/mm	200
Counterweight Rod Mass/g	62

Table 2: First six modes.

Mode	Description	Frequency,Hz
1	1st vertical bending	1.179
2	2nd vertical bending	7.724
3	3rd vertical bending	22.19
4	1st torquing	22.95
5	1st horizontal bending	27.47
6	4th vertical bending	44.27

3.2 Load case for nonlinear coefficients identification

The load case should be selected to activate the nonlinear characters of structure as the input of finite element method (FEM) program, which simulates the dynamic response sample data for nonlinear coefficients identification. This paper adoptes the "3211" multi-level square wave as the input load case, which can adjust Δt to change the frequency rang of the load. The "3211" suqare wave model is presented as

$$\delta=\begin{cases}0 & t\in[0,t_1),t\in[t_1+7\Delta t,+\infty)\\ \alpha & t\in[t_1,t_1+3\Delta t)\\ -\alpha & t\in[t_1+3\Delta t,t_1+5\Delta t)\\ \alpha & t\in[t_1+5\Delta t,t_1+6\Delta t)\\ -\alpha & t\in[t_1+6\Delta t,t_1+7\Delta t)\end{cases} \tag{25}$$

where t is time; t_1 is the start time of the load; α is amplitude of the load. The aerodynamic load of the wing model in the condition of the incoming wind speed of 16m/s and angle of attack of 3° is referred as amplitude of the load. Set $\Delta t=0.1s$, and the effective frequency band of the load is adjusted to cover the natural frequency of 1st vertical bending mode. The power spectral density of the generalized force corresponding to the vertical bending mode and square wave input are shown in Figure 2 and Figure 3. The frequency band is wide, and the energy near the low-frequency bending mode frequency is large, which meets the requirements of dynamic response identification.

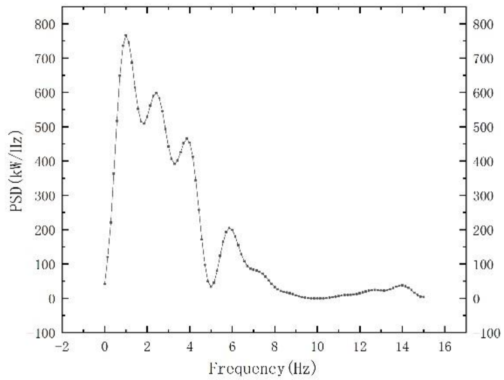

Figure 2: Power spectral density of the generalized force.

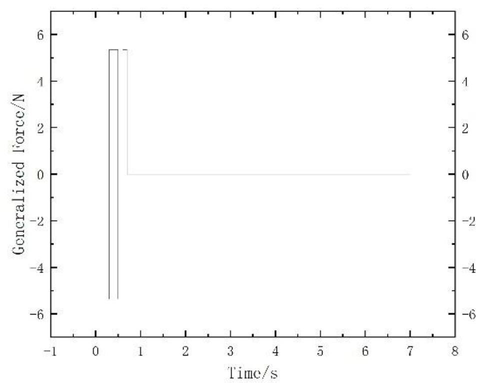

Figure 3: Time domain change of the generalized force.

3.3 Dynamic response simulation based on CR

Co-Rotational finite element (CR FEM) is used to get dynamic response data. Set the stime step as 0.01s, and simulate the dynamic response of 7 seconds as to the model mentioned above. Meanwhile, using the software MSC.Nastran to simulate the dynamic response in the same setting of time step for comparision. The vertical displacement response at the end of wing spar is shown as Figure 4, and the deformation simulated by CR FEM and MSC.Nastran is relatively consistent. However, as is shown in Table 3, CR FEM costs less calculation time to get the results with enough accuracy. Therefore, CR FEM is suitable for providing dynamic response data for nonlinear coefficient identification for its moderate accuracy and high efficiency.

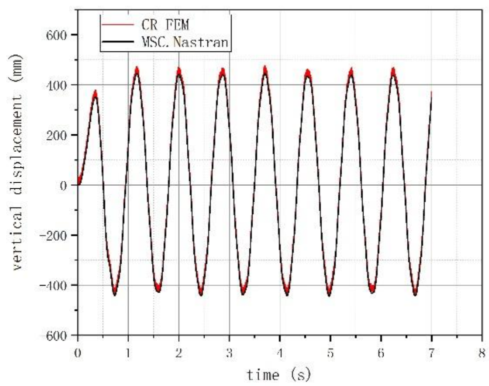

Figure 4: Dynamic response of vertical displacement of wing tip.

Table 3: Time cost of calculation.

Method	Total time cost,s
CR FEM	340
MSC.Nastran	490

3.4 CR-ROM

3.4.1 Static verification

The accuracy of ROM based on CR FEM is verified through static deformation simulation of the wing model, and the aerodynamic load under the condition of angle of attack of 3° and the incoming wind speed of 10m/s, 16m/s and 22m/s respectively is used as the validation load. The results obtained by ROM and by MSC.Nastran are shown in the Figure 5 and Figure 6, where CR-ROM represents the results obtained by ROM (based on the CR FEM); Nonlinear FEM represents the results obtained by MSC.Nastran (SOL 106); Linear FEM represents the results obtained by MSC.Nastran (SOL101).

Figure 5 indicates that the vertical displacement at the end of wing spar obtained by ROM is close to the results of MSC.Nastran. And when the wind speed increases, the deformation increases rapidly, and the ROM results are closer to the nonlinear FEM results than the linear FEM results in the case of large deformation, which show the moderate accuracy of ROM.

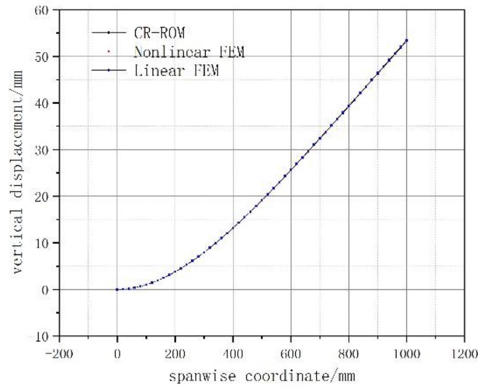

(a) wind speed = 10m/s

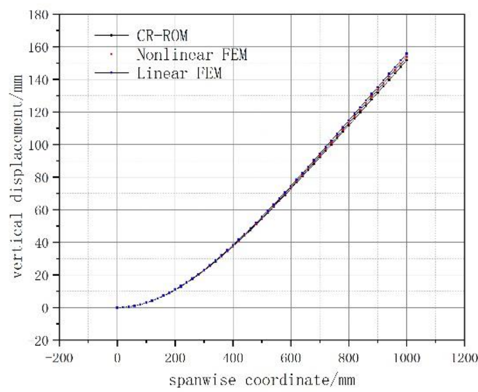

(b) wind speed = 16m/s

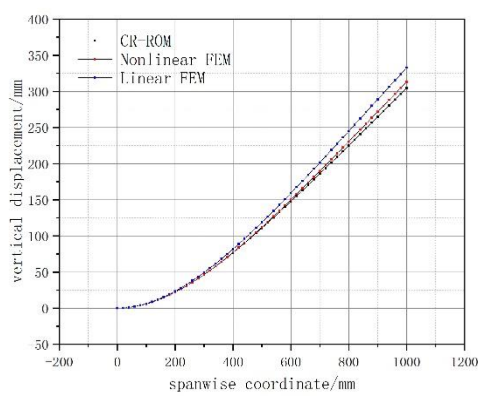

(c) wind speed = 22m/s

Figure 5: Vertical displacement at the end of wing spar at different wind speeds.

Figure 6 shows the huge deviation of linear results from nonlinear FEM results and ROM results in the spanwise deformation. This is because that nonlinear FEM and ROM consider the difference of geometrical configuration before and after deformation. At the wind speed of 22m/s, the spanwise deformation have reached 6% of the semispan, which already has nonnegligible impact on the aerodynamic simulation. Therefore, the nonlinear method for structure is significant for aeroelastic analysis.

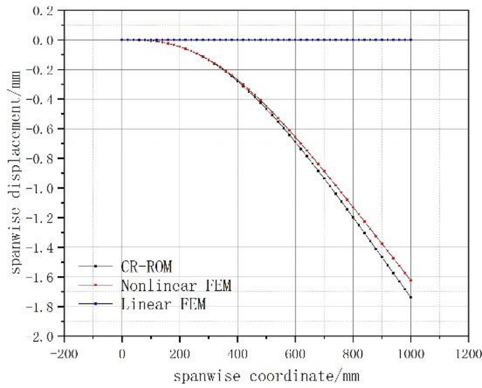

(a) wind speed = 10m/s

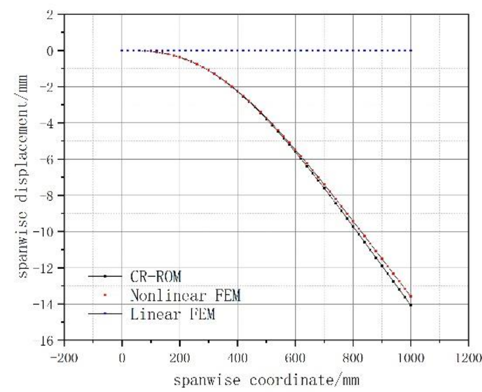

(b) wind speed = 16m/s

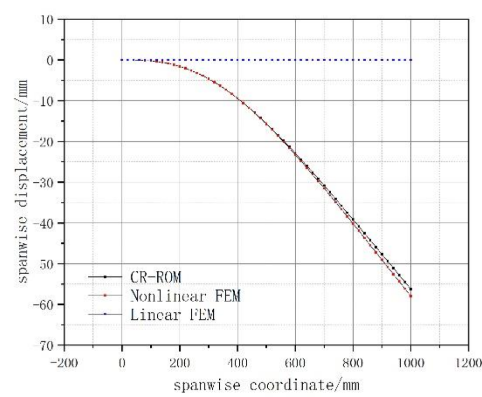

(c) wind speed = 22m/s

Figure 6: Spanwise displacement at the end of wing spar at different wind speeds.

3.4.2 Static aeroelastic analysis

Based on the ROM, the nonlinear static aeroelastic analysis is established. The method is used to perform static aeroelastic analysis on the wing model above, where the vortex lattice method divides the aerodynamic grids into 20 spanwise and 2 chordwise grids, and the angle of attack is set as 3°, and the convergency condition is set as η=0.5mm. As a comparison, the other two methods, nonlinear static aeroelastic analysis method based on nonlinear FEM and vortex lattice method, as well as the linear aeroelastic method, calculate the static aeroelastic deformation of the wing model under the same operating conditions.

The static aeroelastic vertical displacement at the end of wing spar obtained by three methods is shown in Figure 7. As the wind speed get higher, the difference between results obtained by linear static aeroelastic and by nonlinear FEM coupled with VLM is more obvious. And ROM coupled with VLM maintain a high consistency with nonlinear FEM coupled with VLM in the static aeroelastic vertical displacement.

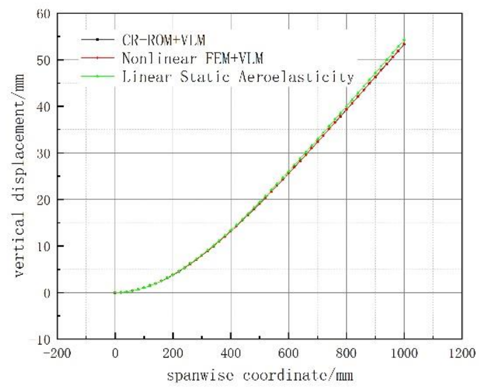

(a) wind speed = 10m/s

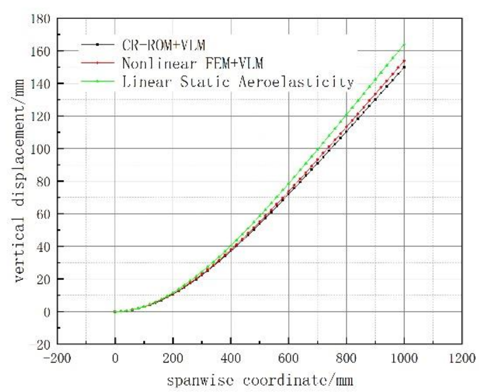

(b) wind speed = 16m/s

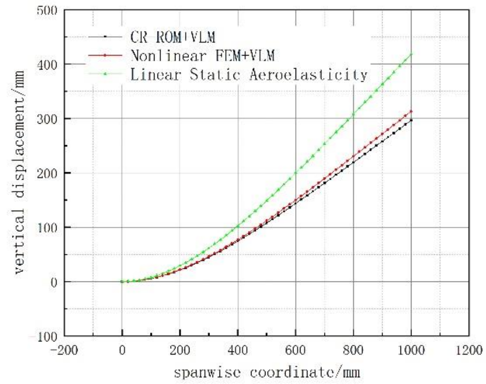

(c) wind speed = 22m/s

Figure 7: Static aeroelastic vertical displacement the end of wing spar at different wind speeds.

The static aeroelastic spanwise displacement at the end of wing spar obtained by three methods is shown in Figure 8. Compaerd to the linear static aeroelastic method, which can not calculate spanwise deformation, the ROM coupled with VLM can get theaccurate results of spanwise deformation. The difference between the results obtained by ROM coupled with VLM and by nonlinear FEM coupled with VLM is within the range of 7%.

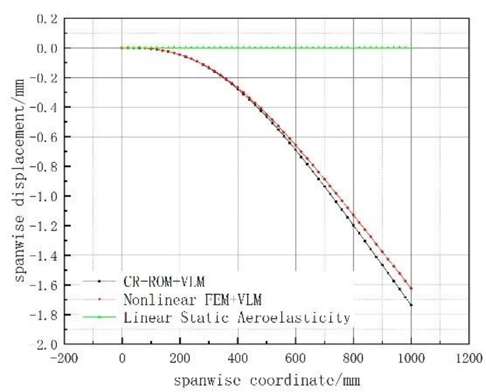

(a) wind speed = 10m/s

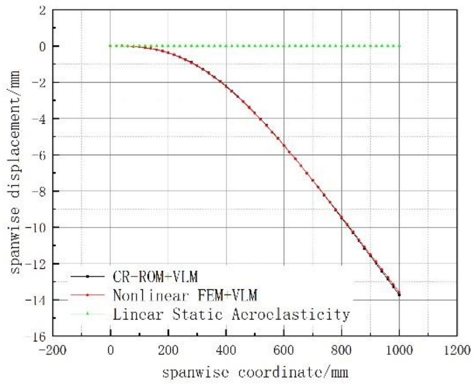

(b) wind speed = 16m/s

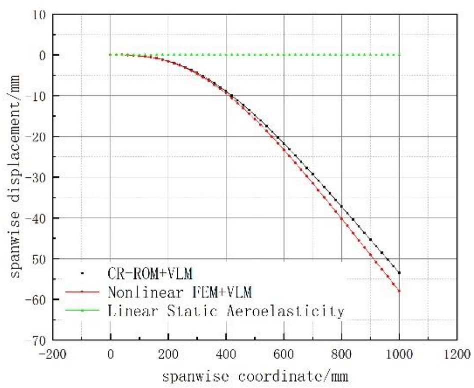

(c) wind speed = 22m/s

Figure 8: Static aeroelastic spanwise displacement at the end of wing spar at different wind speeds.

According to the vertical and spanwise displacement obtained by three methods, compared with the static aeroelastic analysis method based on nonlinear FEM, the aeroelastic analysis method based on the ROM has higher consistency in calculation results, while there is a significant difference between the linear aeroelastic analysis results and the nonlinear method analysis results. ROM can be effectively applied to predict wing structural deformation and nonlinear aeroelastic analysis.

4 CONCLUSIONS

This paper establishes nonlinear dynamic equations and reduced order model for large flexible structures, and uses Harmonic Balance Method and fast Fourier transform parameter identification frequency domain method to build the reduced order model based on dynamic response data samples obtained by CR FEM. And static verification is conducted on the nonlinear ROM method. Through static verification, the nonlinear ROM has the higher accuracy compared with linear method especially in calculation of the spanwise deformation. Combining the ROM and VLM, the nonlinear static aeroelastic method is set up. In the static aeroelastic analysis, the nonlinear static aeroelastic method based on ROM has a relatively close accuracy to that based on nonlinear FEM. Therefore, the ROM based on CR FEM is effective in the nonlinear structure deformation simulation and nonlinear static aeroelastic analysis.

REFERENCES

[1] McEwan, M. I., Wright, J. R., Cooper, J. E., et al. A combined modal/finite element analysis technique for the dynamic response of a non-linear beam to harmonic excitation. *Journal of Sound and Vibration*, 2001, *243(4)*, 601-624.
[2] Mignolet, M. P., Soize, C. Stochastic reduced order models for uncertain geometrically nonlinear dynamical systems. *Computer Methods in Applied Mechanics and Engineering*, 2008, *197(45-48)*: 3951-3963.
[3] Harmin, M. Y., Cooper, J. E., Aeroelastic behaviour of a wing including geometric nonlinearities. *The Aeronautical Journal*, 2011, *115(1174)*: 767-777.
[4] Xie, C., An, C., Liu, Y., et al. Static aeroelastic analysis including geometric nonlinearities based on reduced order model. *Chinese Journal of Aeronautics*, 2017, *30(2)*, 638-650.
[5] An, C., Yang, C., Xie, C., et al. Gust load alleviation including geometric nonlinearities based on dynamic linearization of structural ROM. *International Journal of Aerospace Engineering*. 2019.
[6] Medeiros, R. R., Cesnik, C. E. S., Coetzee, E. B. Computational aeroelasticity using modal-based structural nonlinear analysis. *AIAA Journal*, 2020, *58(1)*, 362-371.
[7] Rankin, C.C., Nour-Omid, B., The use of projectors to improve finite element performance. *Computers Structures*, 1988, *30*, 257-267.
[8] Liu, Y. *Aeroelastic stability and dynamic response analysis of large flexible aircraft*. Beijing: Beihang University (in Chinese), 2016.

COPYRIGHT STATEMENT

The authors confirm that they, and/or their company or organisation, hold copyright on all of the original material included in this paper. The authors also confirm that they have obtained permission from the copyright holder of any third-party material included in this paper to publish it as part of their paper. The authors confirm that they give permission, or have obtained permission from the copyright holder of this paper, for the publication and public distribution of this paper as part of the IFASD 2024 proceedings or as individual off-prints from the proceedings.